Pergamon

Chemical Engineering Science, Vol. 52, Nos. 21/22, pp. 3909–3917, 1997
© 1997 Elsevier Science Ltd. All rights reserved
Printed in Great Britain

PII: S0009-2509(97)00273-X

0009-2509/97 $17.00 + 0.00

Mass transfer in an external-loop airlift reactor: experiments and modeling

H. Dhaouadi,*† S. Poncin,*‡ J. M. Hornut,*† G. Wild,* P. Oinas§ and J. Korpijarvi‖

*Laboratoire des Sciences du Génie Chimique, CNRS ENSIC INPL BP-451, 1 – rue Grandville, 54000 Nancy, France; †Université Henri Poincaré de Nancy, IUT Le Montet, France; §Kemira Fine Chemicals Oy, Kokkola, Finland; ‖Kemira Chemicals Oy, Oulu Research Center, Oulu, Finland

(Accepted 18 July 1997)

Abstract—The mass transfer in an airlift reactor is modeled using simple elementary models: the liquid flow in the riser and the downcomer is represented as plug flow with axial dispersion, while the gas–liquid separator and the bottom junction are considered as CSTRs for the liquid. The gas flow in the riser is represented as plug flow. The system of differential equations resulting from the mass balances applied to the different sections of the reactor are solved in the real-time domain using a commercial software (MODEST). The model parameters are evaluated by adjusting the variation with time of experimental and simulated oxygen concentration profiles in the reactor after change from deoxygenation to oxygenation of the recirculating liquid (dynamic method), at six different locations in the riser, gas-liquid separator and downcomer. The model is tested using experimental data obtained with advanced measuring techniques in a pilot airlift reactor. The data agree well with some correlations from literature.
© 1997 Elsevier Science Ltd

INTRODUCTION

Mass transfer is one of the most important design parameters of gas–liquid reactors for either chemical or biochemical applications. The reactor should have a maximum mass transfer rate, with efficient mixing, at minimum energy input. Several studies have demonstrated the external loop airlift reactor's ability to provide high mass transfer and efficient mixing, but data in the literature for mass transfer vary widely and are sometimes contradictory. Various methods for the mass transfer calculations on the basis of the use of the dynamic method have been published. Almost all the previous works take into account the pressure effect on gas solubility, especially for tall columns; few of them take into account the axial dispersion of the liquid phase, and nearly all of them neglect the oxygen depletion of the gas phase: the above-mentioned studies do not consider the development of oxygen concentration profiles, neither in the liquid nor in the gas phase, due to circulation in the different sections of the reactor. The aims of this paper are, starting from first principles, to introduce a general reactor model for both the gas and liquid phases, taking all these effects into account, and, secondly, to use the derived model for the determination of the essential parameters based on measured data of an airlift reactor.

GENERALIZED CONSERVATION EQUATIONS FOR MULTIPHASE SYSTEMS

An airlift reactor is a quite complicated piece of equipment since it consists of a riser, a downcomer, a gas–liquid separator at the top and a junction between the downcomer and the riser. All the model equations are derived using principal Navier–Stokes equations, following the principles given, e.g. by Hillmer *et al.* (1994) for slurry bubble columns. The models are written for one velocity direction only ignoring radial effects.

The basic equation in phase k is

$$\frac{\partial(\rho\varepsilon\Phi)_k}{\partial t} = -\frac{\partial}{\partial z}(\rho\varepsilon U\Phi)_k + \frac{\partial}{\partial z}\left(\frac{\mu_{\text{eff}}}{\sigma}\varepsilon\frac{\partial\Phi}{\partial z}\right)_k + S_\Phi. \quad (1)$$

In this paper, we show the implementation of a reduced model, using common axial dispersion model for the riser, plug-flow model for the downcomer and CSTR-models for the junction stagers. The development of (1) utilizing also balances for axial momentum results in the equations of Table 1 for the holdups, velocities and concentrations describing the flows and mass transfer (Dhaouadi, 1997; Korpijarvi, 1997; and Oinas, 1996) in an airlift reactor. Gas flow is assumed to follow plug flow patterns in both the riser and

‡Corresponding author. Tel.: 33 383 175223; fax: 33 3833 229 75; e-mail: poncin@ensic.u-nancy.fr.

Table 1. Developed equation system used for flow and mass transfer description in an airlift reactor (Korpijarvi, 1997)

Term	Liquid		Gas	
ε	$\varepsilon_l = 1 - \varepsilon_g$	(2)	$\frac{\partial \varepsilon_g}{\partial t} = -\left(u_g \frac{\partial \varepsilon_g}{\partial z} + \varepsilon_g \frac{\partial u_g}{\partial z}\right) - k_l a (C_l^* - C_l) \frac{M_w}{\rho_l}$	(3)
u	$\frac{\partial u_l}{\partial t} = -u_l \frac{\partial u_l}{\partial z} + \frac{2D}{\varepsilon_l} \frac{\partial \varepsilon_l}{\partial z} \frac{\partial u_l}{\partial z} + \frac{1}{\rho_l} \frac{\partial P}{\partial z} - (1 - \lambda_l) g \pm \frac{\varepsilon_g u_l C_w}{\varepsilon_l \rho_l} \quad \lambda_l = \frac{\rho_{sus}}{\rho_l}$	(4)	$\frac{\partial u_g}{\partial t} = -u_g \frac{\partial u_g}{\partial z} + \frac{2D}{\varepsilon_g} \frac{\partial \varepsilon_g}{\partial z} \frac{\partial u_g}{\partial z} + \frac{1}{\rho_g} \frac{\partial P}{\partial z} - (1 - \lambda_g) g \pm \frac{u_l C_w}{\rho_g} \quad \lambda_g = \frac{\rho_{sus}}{\rho_g}$	(5)
C	$\frac{\partial C_l}{\partial t} = -u_l \frac{\partial C_l}{\partial z} + D\left(\frac{1}{\varepsilon_l} \frac{\partial \varepsilon_l}{\partial z} \frac{\partial C_l}{\partial z}\right) + D\left(\frac{\partial^2 C_l}{\partial z^2}\right) + k_l a (C_l^* - C_l) \frac{M_w}{\rho_l} C_l$	(6)	$\frac{dy}{dt} = \left[-u_g + D\left(\frac{1}{\varepsilon_g} \frac{\partial \varepsilon_g}{\partial z} + \frac{2}{P} \cdot \frac{\partial P}{\partial z}\right)\right] \frac{\partial y}{\partial z} + D \frac{\partial^2 y}{\partial z^2} + y \frac{1}{P} \frac{\partial P}{\partial z}\left(-u_g + D \frac{1}{\varepsilon_g} \frac{\partial \varepsilon_g}{\partial z}\right) - k_l a (C_l^* - C_l) \frac{M_w}{\rho_l} y$	(7)

Table 2. Equation system used for the description of flow and mass transfer in the external loop airlift reactor (Dhaouadi, 1997)

Phase	Liquid		Gas	
Riser		(6)	$\frac{dy}{dt} = -u_g \frac{\partial y}{\partial z} - u_g y \frac{1}{P} \frac{\partial P}{\partial z} - k_l a (C_l^* - C_l) \frac{M_w}{\rho_l} y$	(7)
Gas–liquid PMR1 Separator	$\frac{dc_l}{dt} = \frac{Q_l}{(1 - \varepsilon_g) V} (c_{le} - c_l) + \frac{k_l a}{(1 - \varepsilon_g)} (c^* - c_l)$	(8)	$\frac{dc_g}{dt} = \frac{Q_g}{\varepsilon_g V} (c_{ge} - c_g) - \frac{k_l a}{\varepsilon_g} (c^* - c_l)$	(9)
PMR2	$\frac{dc_l}{dt} = \frac{Q_l}{V_{PMR2}} (c_{le} - c_l)$	(10)	Neglected	
Downcomer	$\frac{\partial c_l}{\partial t} = -u_l \frac{\partial c_l}{\partial z}$	(11)	Neglected	
Bottom junction	$\frac{dc_l}{dt} = \frac{Q_l}{V_{PMR3}} (c_{le} - c_l)$	(12)	Neglected	

downcomer. Table 2 presents the conventional equations used for the present study.

EXPERIMENTAL INVESTIGATION

Experiments were carried out in an airlift loop reactor with a height of 6 m (Fig. 1). The diameters of the riser and downcomer are 150 and 81.4 mm, respectively; the liquid is water and the gas feed can be switched from air to nitrogen or *vice versa*; the oxygen concentrations are measured at six different levels in either riser and downcomer by Clark probes connected to a data-acquisition system.

At the column height used here, it is not any longer possible to ignore the effect of the column height on the solubility: static pressure causes a decrease by a factor of 1.6 of the solubility between the bottom and the top of the riser. In case of a classical bubble column (without downcomer), this leads to an increase of the dissolved oxygen concentration in the lower part of the column, and a decrease in the upper part (schematically shown in Fig. 2). In case of an airlift reactor, the movement of the liquid caused by the air-lift effect, homogenizes the liquid, which explains the solubility levels c_∞ observed in the loop reactor for different axial positions (Fig. 3).

The unsteady-state gassing-in method is used for $k_l a$ determination; it is technically very easy and gives, if well analyzed, reliable results. Omitting the considerations mentioned above (especially about the static height effect) would have resulted in major errors in the determination of $k_l a$.

MODELING AND RESULTS

The model of the airlift reactor system was formulated by dividing it into four sections: riser, gas–liquid separator, downcomer and bottom junction.

Referring to Table 2, the flow of the gas phase in the riser can be considered as plug flow, as shown clearly by the gas phase RTD (Fig. 4).

Concerning the liquid phase, the flow in the riser is plug flow with axial dispersion, the downcomer is considered as a plug flow column and the remaining two sections as CSTRs with and without bubbles, respectively.

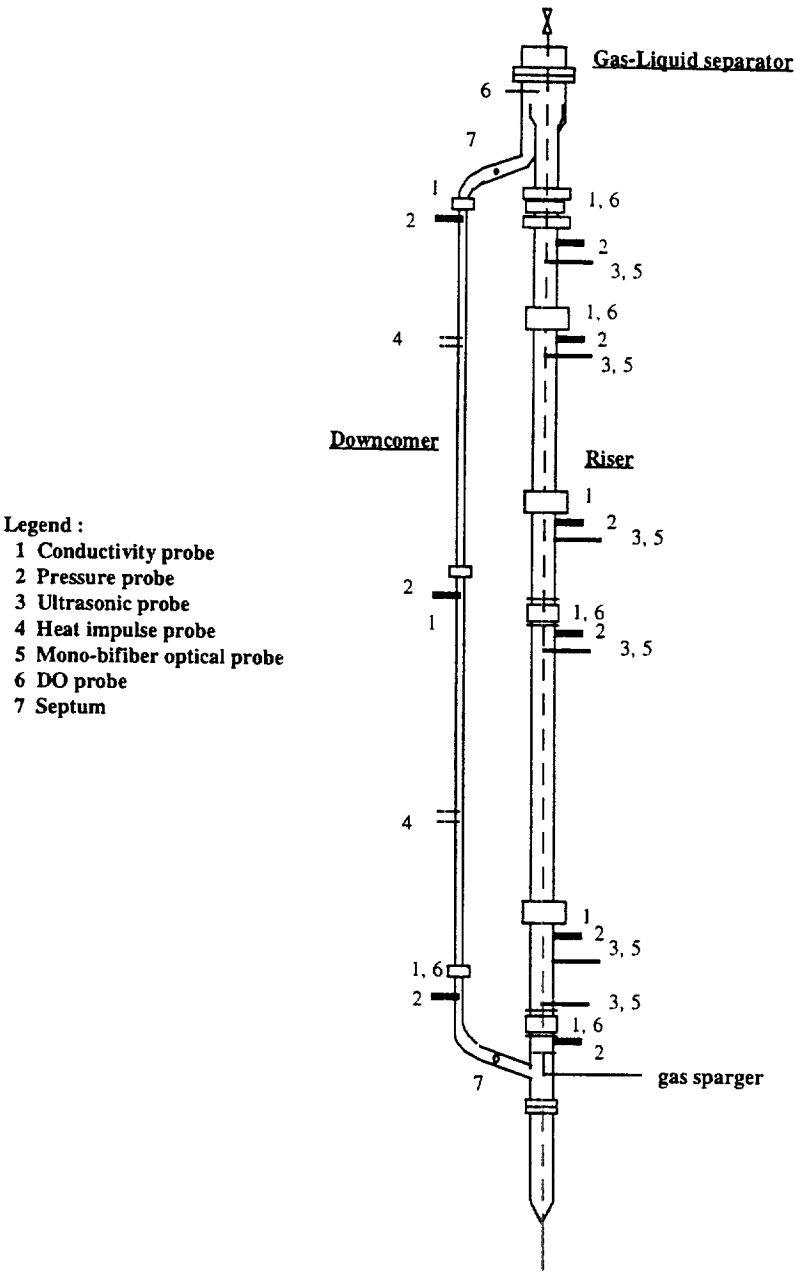

Fig. 1. Experimental set-up.

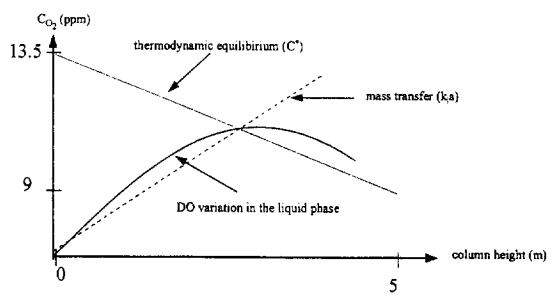

Fig. 2. Mass transfer effects and thermodynamic equilibrium on oxygen solubility.

The elementary models used to describe the hydrodynamic behavior of each region of the external-loop airlift reactor are described in Fig. 5; they show a good agreement with experimental data (Dhaouadi *et al.*, 1996) obtained by the salt-tracer injection techniques (Fig. 6). The nonhomogeneity of the liquid in this complex system appears clearly at small time scales (less than 100 s); at time scales larger than a few dozens of seconds, the liquid can, as a first approximate, be considered as perfectly mixed. Beside the balance equations of Table 2, the response time of the oxygen probes has to be taken into account. This leads to a set of first-order differential equations

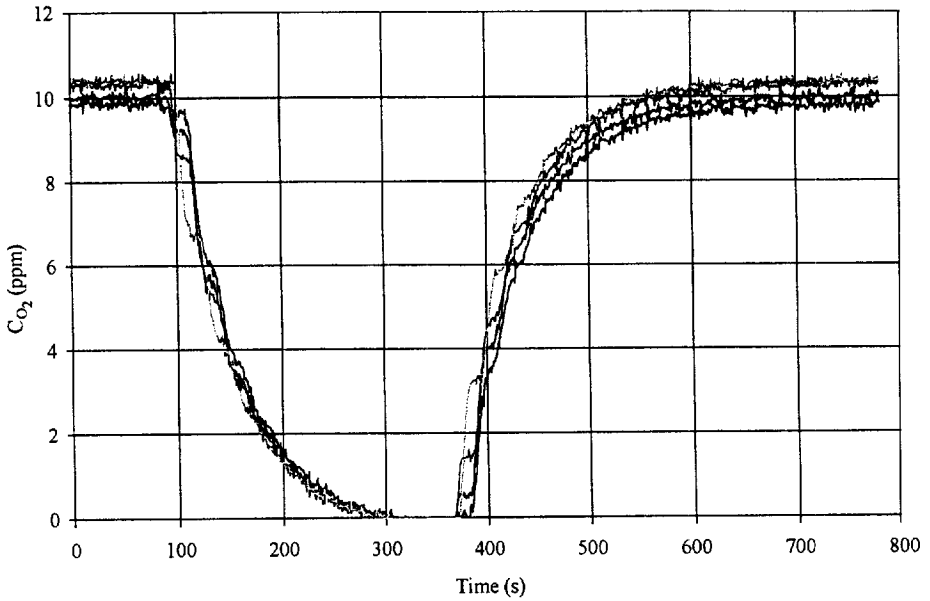

Fig. 3. Typical response of the oxygen probes placed in the riser.

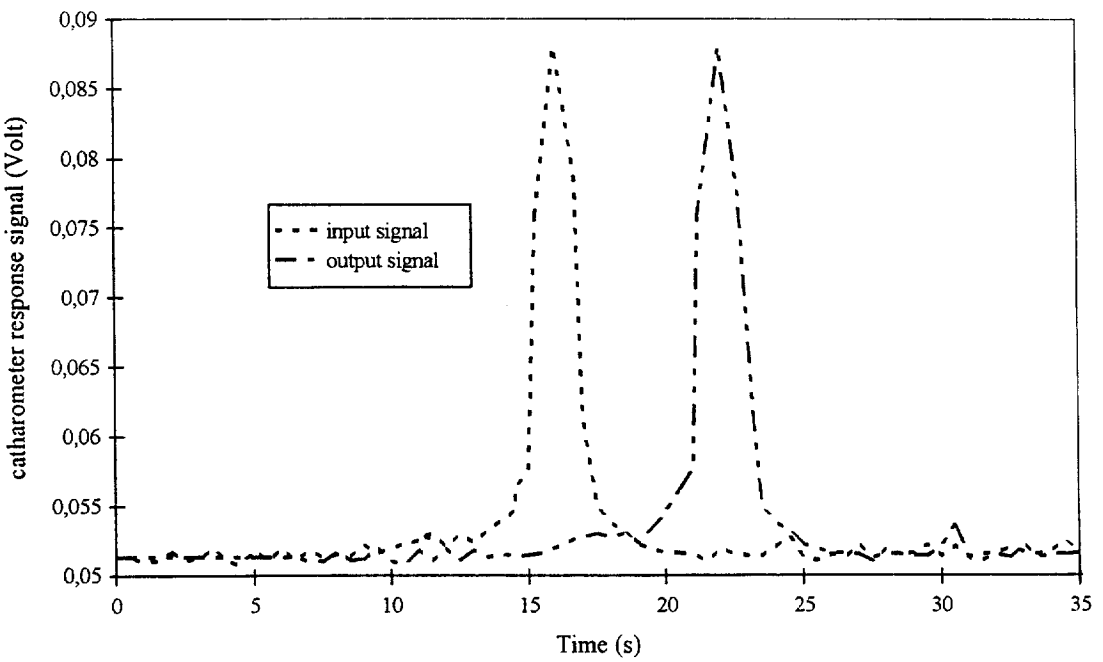

Fig. 4. RTD of the gas phase in the used reactor measured by the mean of a catharometer.

which have to be solved simultaneously with the balance equations of Table 2.

PARAMETER ESTIMATIONS

In order to estimate the parameters of the model, a set of ordinary (ODE) and partial second-order differential equations (PDE) have to be solved; MODEST® program package (Haario, 1994) was employed: for solving the PDEs for the riser, the column section is first discretised into 40 subsections and by employing the method of lines (Schiesser, 1991) the obtained ODEs are integrated in time. The differential equations are solved with LSODE (Hindmarsh, 1983). The downcomer is discretized into 10 subsections. The presence of gas in the downcomer is neglected which corresponds to our experiments with water. With viscous or noncoalescing liquids the gas entrainment in the downcomer can no longer be neglected; in that case, the liquid and gas-phase balances in the downcomer and take the same form as in the riser and

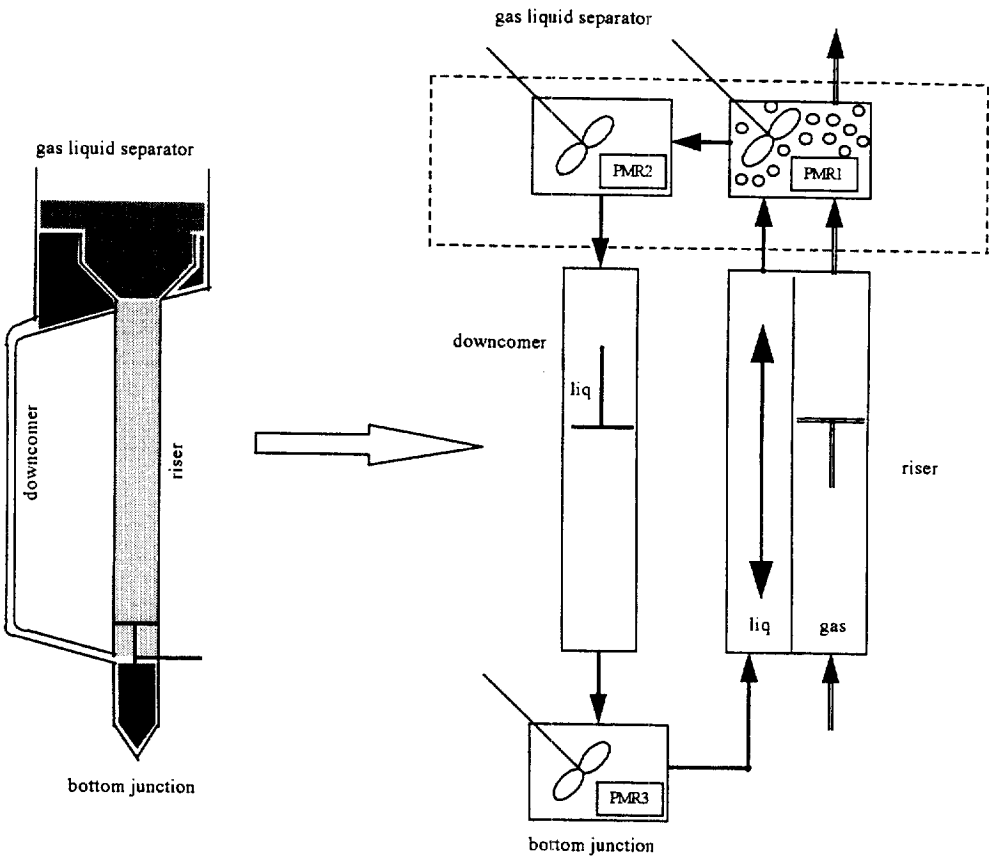

Fig. 5. Elementary models used for mass transfer description in the external-loop airlift reactor.

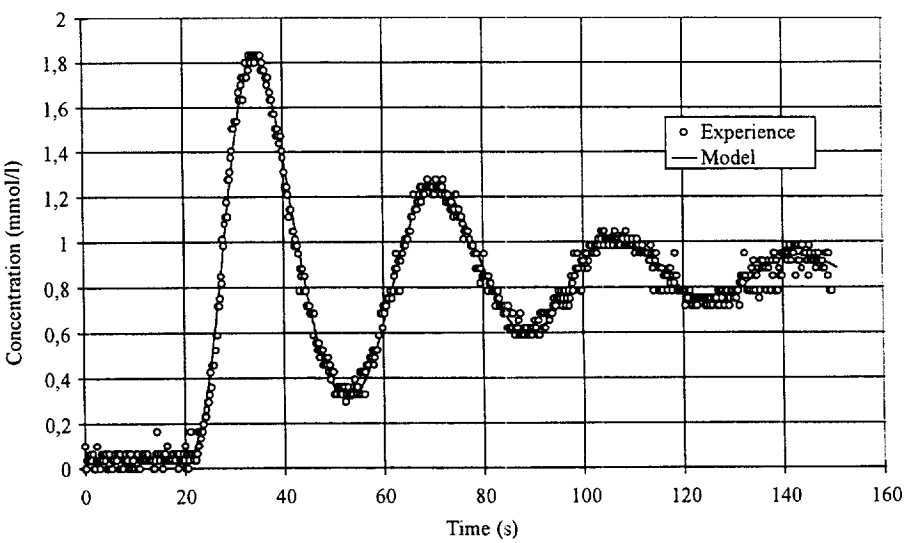

Fig. 6. Fitting example of a response to a tracer injection in the reactor used (hydrodynamic model).

the computational times are substantially increased. The results presented here all concern water.

The objective function is minimized by the simplex method in parameter estimations. The closeness of the data and the values predicted by the model can be measured, in principle, with several criteria. The most common objective function according to which the parameters are estimated is the sum of residual squares. The quality of fit is characterized by the coefficient of determination, R^2.

The parameters to be estimated in this study were the volumetric coefficient of gas–liquid mass

transfer, $k_l a$, and the dispersion coefficients in the riser, D.

The gas holdup and liquid velocity figures are taken from separate measurements described elsewhere (Dhaouadi, 1997).

RESULTS AND DISCUSSION

Most experiments were made by switching the gas feed from nitrogen to air; in some experiments, the feed was switched from air to nitrogen. Figure 7 shows such a deoxygenation followed by a re-oxygenation of the water, with a curve corresponding to a single $k_l a$ value. It is clear that $k_l a$ does not depend on the direction of the mass transfer.

Due to the time scale of Fig. 7, the behavior of the liquid can, in first approximation be considered as that of a CSTR. Figure 8 gives a more detailed representation of an oxygen probe in the riser. One sees clearly in this figure the different steps corresponding to the recirculation of the liquid. Similar curves were obtained with all the oxygen probes. All these curves could be fitted with a single set of parameters $k_l a$ and D. The quality of the fit is illustrated on Fig. 8.

The transfer rate, $k_l a(c^* - c_1)$, in the used equations is always changing with both space and time: c^* due to the pressure effect on oxygen solubility and c_l because of oxygen mass transfer. In fact, $k_l a$ is also changing during time; its variation is bigger in the beginning and the value of $k_l a$ considered is a mean value in time (its variation in space is negligible). In the derivative term dc_l/dt, the biggest changes occurs during the first 50 s because of the maximum

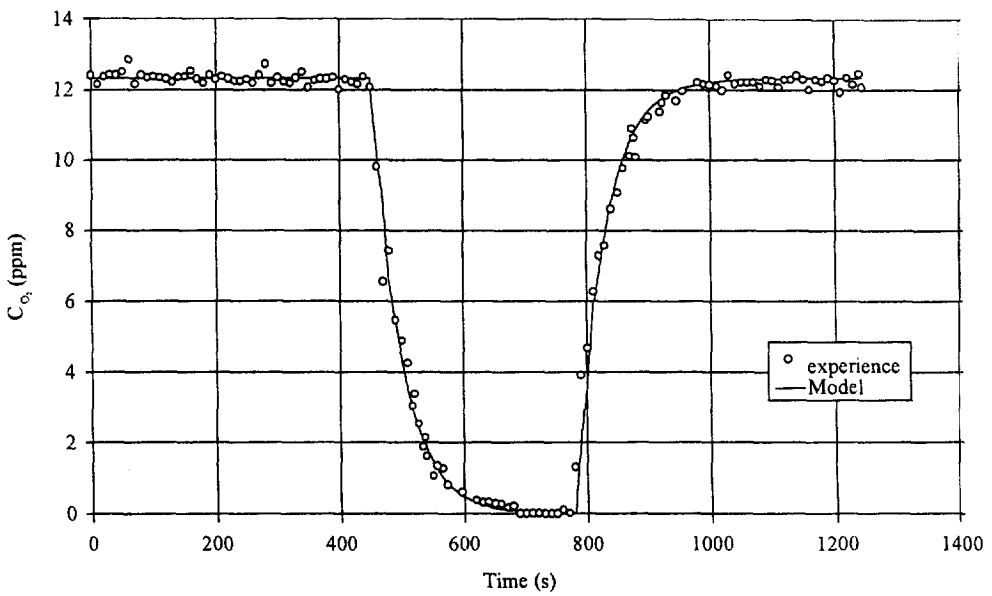

Fig. 7. Fitting example of the oxygen probe response during the deoxygenation/oxygenation period.

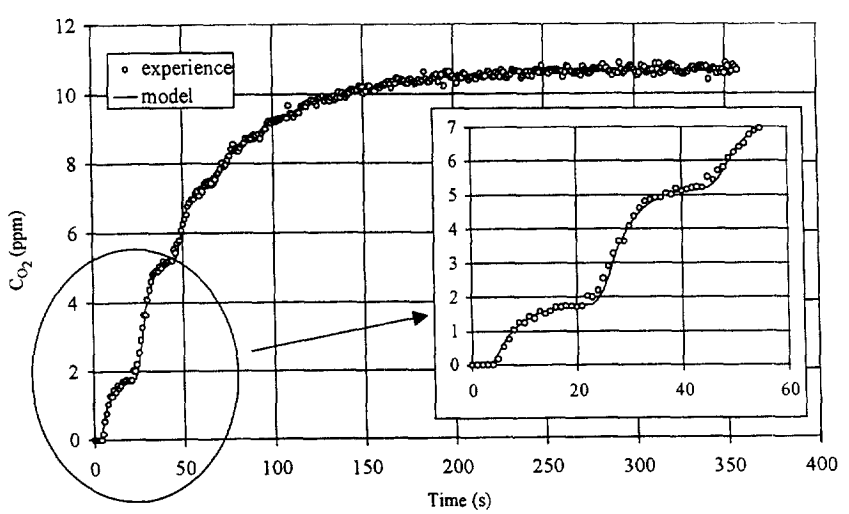

Fig. 8. Fitting example of the oxygen probe response during the oxygenation period.

difference in the $(c^* - c_1)$ term. Having optimized the mean values of the parameters, it is possible to get the development of dissolved oxygen concentrations in the liquid phase at each level of the reactor (Fig. 9).

Beside the numerical solution, an original exact analytical solution assuming axial dispersion, plug flow and CSTR behavior was also developed for k_la calculation. The analytical solution presented elsewhere (Dhaouadi, 1997) is, however, quite cumbersome. Figure 10 shows the agreement between the numerical solution of the proposed model and the analytical one.

The model contains two parameters: the axial dispersion coefficient and the mass transfer coefficient k_la, the values of which may not be independent. This effect was studied by analyzing the sensitivity of the proposed model to the variations around the optimum of the objective function.

Figure 11 shows that, compared to k_la, the axial dispersion coefficient cannot be identified. Indeed, imposing a zero value of D or keeping it as a model parameter when comparing the experimental data to the model yields nearly the same value of optimized k_la. Beside the comparison of the analytical and numerical solutions, Fig. 10 illustrates also the moderate influence of the axial dispersion coefficient on k_la. The simple model used here cannot present exact values for both of the parameters. The values of the mass transfer coefficient obtained were compared with all the correlations available. The best fits were obtained with the correlations represented in Fig. 12. The results obtained show a good agreement with both

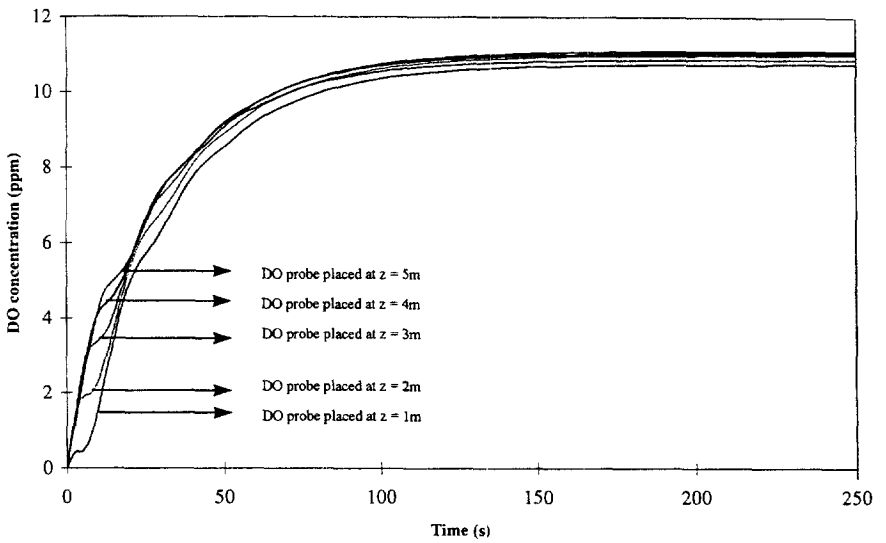

Fig. 9. Example of simulation of oxygen probe response in external-loop airlift reactor.

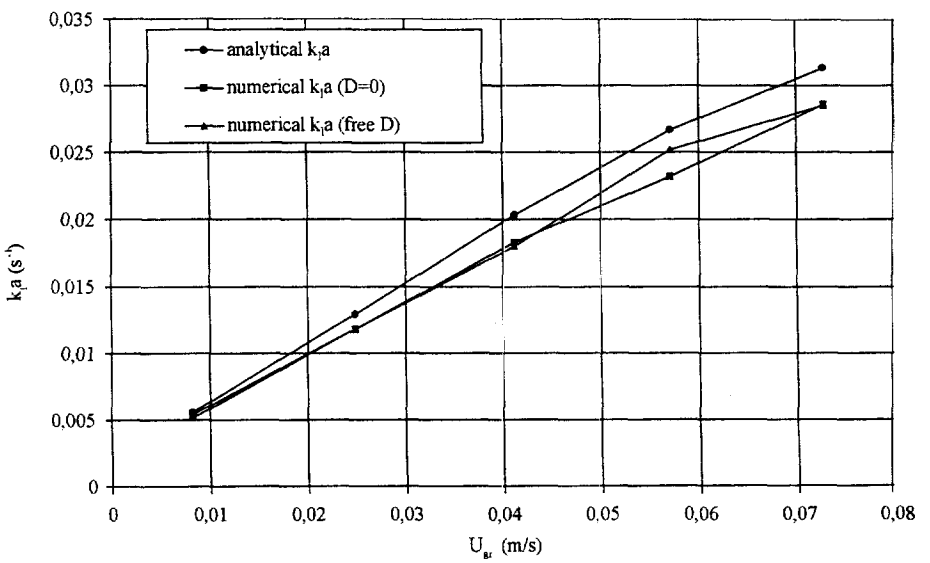

Fig. 10. Axial dispersion effects on k_la values in the reactor used.

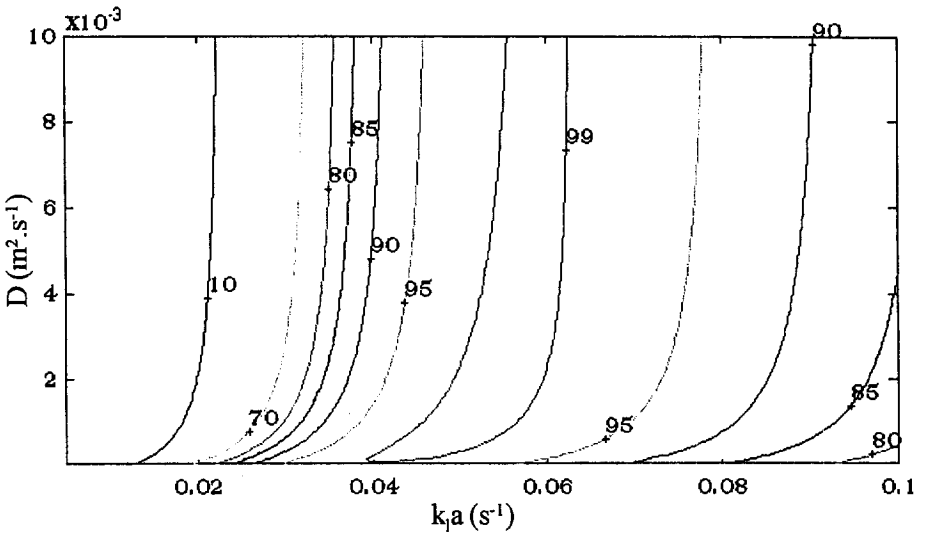

Fig. 11. Sensitivity (R^2 values) of the model used to k_la and D variations in airlift loop reactors.

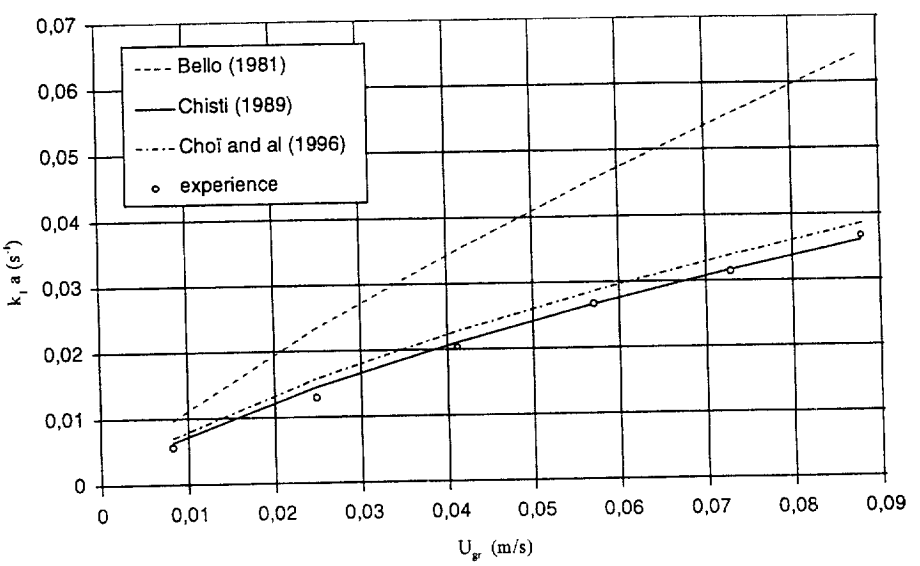

Fig. 12. Comparison of the experimental results with the existing correlation.

correlation of Chisti (1989) and Choi *et al.* (1996). The correlation proposed by Bello (1981) overestimates the gas effect on k_la.

CONCLUSIONS

In dynamic modeling of multiphase reactors, often comparison of the predictions of the model with experiments is done in the Fourier or Laplace domain. Furthermore, in the investigation of air-lift reactors, usually, the liquid is assumed to be perfectly mixed. Due to the quality of the experimental measurements made here and to the relatively large scale of the equipment used (more than 5 m height), it was possible to discriminate between a more sophisticated model presented here (see the steps in Fig. 8) and the simplistic model usually used in literature. Here, the equations of the model (mass balances in different parts of the equipment) were solved in the time domain, with the use of an efficient software. It has been shown that an intrinsically quite simple model is able to describe the mass transfer behavior of an external loop airlift reactor with a very good precision, specially, it is able to predict in a quite precise way the local and instantaneous values of the concentrations in an airlift reactor, which would not be possible with the usual CSTR approach. It should be very easy to include reaction terms in this model, which already includes gas depletion and static pressure effects on solubility. In case of very slow biochemical reactions, this is not always important, but may play an important role in the design of airlifts as

chemical reactors; then, this model becomes a valuable design tool.

Future work in this field should tackle the following features: improving the hydrodynamic model by using CFD codes; checking the influence of the initial gas distribution and of the physical properties of the liquid.

NOTATION

$\bar{y}$	average value of all data points
C	concentration, mol m^{-3}
C_w	drag force, kg m^{-3} s^{-1}
D	axial dispersion coefficient, m^2 s^{-1}
DO	dissolved oxygen, ppm
g	gravitational force, m s^{-2}
$k_l a$	volumetric mass transfer coefficient, s^{-1}
M_w	molecular weight, kg mol^{-1}
P	pressure, Pa
Q	flow rate, m^3 s^{-1}
R^2	coefficient of determination $100 \times \left(1 - \frac{\lvert y - y_p \rvert^2}{\lvert y - \bar{y} \rvert^2}\right)$
RTD	residence time distribution
S_Φ	source term
T	temperature, K
t	time, s
u	axial velocity, m s^{-1}
V	volume, m^3
y (in eq. (7))	molar fraction
y (in R^2)	data point value
y_p	prediction given by the model
z	distance coordinate, m

Greek letters

ρ	density, kg m^{-3}
μ_{eff}	effective viscosity, Pa s
ε	hold-up
λ	density ratio
Φ	variable of eq. (1)
σ	Schmidt number ($= \mu_{\text{eff}}/\rho D_{\text{eff}}$)

Subscripts and superscripts

e	entrance
g	gas
i	component i
k	phase k
l	liquid
sus	suspension
*	equilibrium state

REFERENCES

Bello, R. A. (1981) A characterization study of airlift contactors for applications to fermentation. Ph.D. thesis, University of Waterloo, Ontario.

Chisti, M. Y. (1989) *Airlift Bioreactors*. Elseiver Applied Science, London and New York.

Choi, K. H., Chisti, Y. and Moo-Young, M. (1996) *Biochem. Engng J.*, **62**, 223–229.

Dhaouadi, H. (1997) Etude d'un réacteur à gazosiphon à recirculation externe. Ph.D. thesis, Institut National Polytechniques de Lorraine (INPL), Nancy, France.

Dhaouadi, H., Poncin, S., Hornut, J. M., Wild, G. and Oinas, P. (1996) *Chem. Engng Sci.* **51**, 2625–2630.

Haario, H. (1994) *MODEST User's Guide*, Helsinki, Finland.

Hillmer, G., Weismantel, L. and Hofmann, H. (1994) *Chem. Engng Sci.* **49**, 837.

Hindmarsh, A. (1983) ODEPAK, A systematic collection of ODE solvers. In *Scientific Computing*, eds. R. S. Stepleman *et al.*, IMACS North-Holland, Amsterdam.

Korpijarvi, J. (1997) The hydrodynamics and mass transfer of an internal loop airlift reactor. M.Sc. Thesis, Lappeenranta University of Technology, Lappeenranta, Finland.

Oinas, P. (1996) Study on the mass transfer and reaction models in multiphase systems, Ph.D. thesis, Acta. Univ. Oul. C94, Oulu Univ. Press, Oulu, Finland.

Schiesser, W. E., (1991) *The Numerical Method of Lines. Integration of Partial Differential Equations.* Academic Press, San Diego, CA.